Clin Neuroradiol (2019) 29:109–115
https://doi.org/10.1007/s00062-017-0636-2

ORIGINAL ARTICLE

Quantitative Rapid Assessment of Leukoaraiosis in CT

Comparison to Gold Standard MRI

Uta Hanning[1,2,3] · Peter Bernhard Sporns[2] · Rene Schmidt[4] · Thomas Niederstadt[2] · Jens Minnerup[5] · Georg Bier[6] · Stefan Knecht[7] · André Kemmling[8]

Received: 8 June 2017 / Accepted: 30 September 2017 / Published online: 20 October 2017

Abstract
Purpose The severity of white matter lesions (WML) is a risk factor of hemorrhage and predictor of clinical outcome after ischemic stroke; however, in contrast to magnetic resonance imaging (MRI) reliable quantification for this surrogate marker is limited for computed tomography (CT), the leading stroke imaging technique. We aimed to present and evaluate a CT-based automated rater-independent method for quantification of microangiopathic white matter changes.
Methods Patients with suspected minor stroke (National Institutes of Health Stroke scale, NIHSS < 4) were screened for the analysis of non-contrast computerized tomography (NCCT) at admission and compared to follow-up MRI. The MRI-based WML volume and visual Fazekas scores were assessed as the gold standard reference. We employed a recently published probabilistic brain segmentation algorithm for CT images to determine the tissue-specific density of WM space. All voxel-wise densities were quantified in WM space and weighted according to partial probabilistic WM content. The resulting mean weighted density of WM space in NCCT, the surrogate of WML, was correlated with reference to MRI-based WML parameters.
Results The process of CT-based tissue-specific segmentation was reliable in 79 cases with varying severity of microangiopathy. Voxel-wise weighted density within WM spaces showed a noticeable correlation (r = –0.65) with MRI-based WML volume. Particularly in patients with moderate or severe lesion load according to the visual Fazekas score the algorithm provided reliable prediction of MRI-based WML volume.
Conclusion Automated observer-independent quantification of voxel-wise WM density in CT significantly correlates with microangiopathic WM disease in gold standard MRI. This rapid surrogate of white matter lesion load in CT may support objective WML assessment and therapeutic decision-making during acute stroke triage.

Keywords Leukoaraiosis · White matter lesions · Cerebral small vessel disease · CT segmentation techniques · Acute stroke

Uta Hanning and Peter Sporns contributed equally to the manuscript.

✉ Uta Hanning
u.hanning@uke.de

1 Department of Diagnostic and Interventional Neuroradiology, Universal Medical Center Hamburg-Eppendorf, Hamburg, Germany

2 Department of Clinical Radiology, University Hospital of Münster, Münster, Germany

3 Department of Epidemiology and Social Medicine, University of Münster, Münster, Germany

4 Institute of Biostatistics and Clinical Research, University of Münster, Münster, Germany

5 Department of Neurology, University Hospital of Münster, Münster, Germany

6 Department of Diagnostic and Interventional Neuroradiology, Eberhard Karls University Tübingen, Tübingen, Germany

7 Department of Neurology, Mauritius Hospital and University Hospital of Düsseldorf, Düsseldorf, Germany

8 Institute of Neuroradiology, University Hospital of Lübeck, Lübeck, Germany

Introduction

White matter lesions (WML) are a common finding in the elderly brain and are primarily caused by cerebral small

vessel disease with the major risk factors hypertension, age and ischemic stroke [1]. This surrogate marker of end organ damage is known to predict poor outcome in stroke patients treated with intravenous thrombolysis [2–5]. A severe WML load increases the risk of hemorrhagic infarct transformation after mechanical thrombectomy and thrombolysis in stroke patients [6, 7]; however, visual rating scales to assess severity of WML are imprecise with high interrater variability and individual prediction of potentially WML-related hemorrhagic events remains unreliable [8]. A more precise and rapid quantification of WML load in the acute stroke setting may improve risk stratification for thrombolysis or endovascular intervention.

Up to now, reliable automated quantification methods only exist for magnetic resonance imaging (MRI) [9, 10] but not for computed tomography (CT) [9], the leading imaging technique in the acute stroke triage [11]. Furthermore, it is uncertain to what extent a T2 hyperintense WM lesion in MRI is congruent with reduced density in CT due to altered tissue attenuation, since these imaging features may not necessarily represent the same histopathological entity. For this reason, we employed and evaluated a previously established rater-independent method for partial volume tissue segmentation in CT images to detect and grade WM changes per voxel. This segmentation algorithm is based on the voxel-wise decomposition of tissue density in Hounsfield units (HU) in CT into brain tissue-specific components [12]. We hypothesized that the reduction of density of the segmented white matter component in NCCT may be used as a surrogate marker for the severity of microangiopathic WML detected by T2 signal change in MRI: therefore, the purpose of this study was to test and evaluate this automated CT-based method for quantification of WM disease in comparison to volumetric and visual burden of WML load detected by the reference standard MRI.

Material and Methods

Patients

To analyze non-contrast computerized tomography (NCCT) and MRI for WML assessment, we retrospectively screened patients admitted for minor symptoms of stroke between December 2013 and 2014 at the University Hospital of Münster, a tertiary stroke center. At our institution, NCCT is part of the routine multimodal stroke protocol (NCCT, CT angiography and CT perfusion) for suspected stroke and admission <6 h after symptom onset. All clinical data were collected from electronic patient files. If no evident infarction or hemorrhage is detected on CT images all patients receive a multimodal MRI stroke protocol, including a fluid attenuated inversion recovery (FLAIR) sequence, within 2 days. The inclusion criteria for this study were: (1) suspected stroke with NIHSS scored <4, (2) NCCT on admission and (3) follow-up MRI performed within 1 week. Reasons for exclusion were (1) poor imaging quality and (2) missing follow-up imaging. All MR and CT images were performed during clinical routine. Patient information and records were anonymized and de-identified prior to analysis and our study design was entirely retrospective.

Imaging

The initial NCCT was performed on a 128-slice CT scanner (SOMATOM Definition Flash; Siemens AG, Forchheim, Germany; NCCT: 120 kV, 340 mA, 5.0-mm slice reconstruction, 1.0 mm increment, 0.6 mm collimation, 0.8 pitch, and H30s soft kernel). Follow-up FLAIR-MRI was performed on a 1.5 T scanner to detect WML (Gyroscan Interna, Philips Medical Systems, Eindhoven, The Netherlands; FLAIR: TR/TE, 8000/120 ms; FOV 23 cm; 256 × 256 matrix).

MRI Segmentation of WML and Fazekas Score

The MRI was the reference standard for the classification and grading of WML severity, which was assessed by visual and qualitative grading and volumetric segmentation. The WML in FLAIR (Fluid-attenuated inversion recovery) images was manually segmented by an experienced neuroradiologist (Software: Analyze 10.0; AnalyzeDirect Inc., Overland Park, KS, USA) to obtain volumetric WML load (ml). To account for variable head size and brain volume, the WML volume was normalized to the total volume of WM space and expressed as the percentage of lesion load within total WM (Fig. 1a). The total volume of WM in MRI was determined by partial volume segmentation of high-resolution T1 images using FAST 4.0 toolbox (FMRIB's Automated Segmentation Tool integrated in FSL software) with manual correction of misclassified WM voxels [13]. All FLAIR images were independently scored by two radiologists (P.S. with 3 years and U.H. 6 years of experience in neuroradiological imaging) using the Fazekas grading scale according to the extent of deep white matter (DWM) leukoaraiosis (LA) associated with chronic small vessel ischemic disease [14]. Images were scored I—III as follows: I punctuate foci (mild), II beginning confluence (moderate) and III large confluent lesions (severe). Fazekas scores of the more experienced radiologist were used as reference standard for visual assessment of WML.

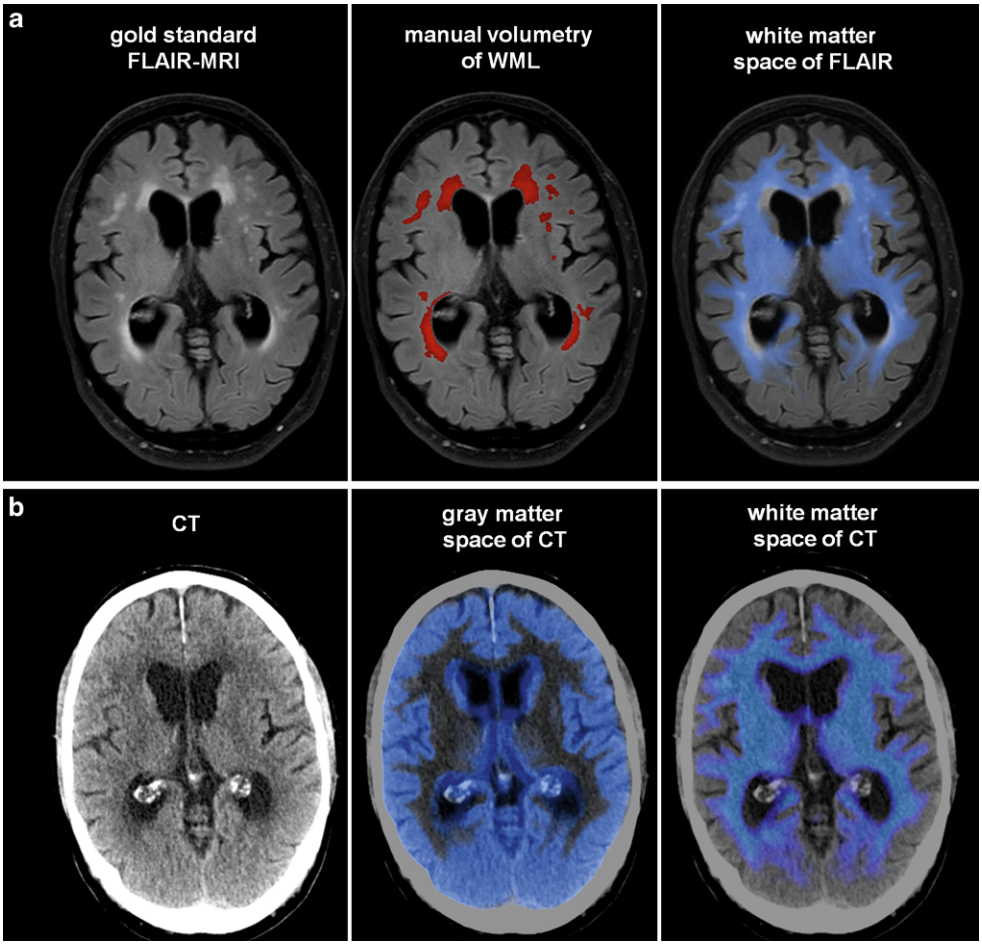

Fig. 1 63-year-old patient with longstanding arterial hypertension and severe LA. **a** *Left*: FLAIR-MRI with T2 hyperintense WML. *Middle*: slice by slice manual segmentation of the WML load in MR FLAIR images (Analyze 10.0). *Right*: WML volume was afterwards normalized to the total volume of WM space defined by probabilistic tissue segmentation. WML load was then expressed as percentage of volume within total volume of WM. **b** *Left*: NCCT co-registered to MRI showing diffuse reduced density of white matter. Probabilistic segmentation of NCCT then defined the partial tissue content per voxel. *Middle*: probabilistic gray matter segmentation. *Right*: probabilistic white matter segmentation. The specific tissue density within WM space was then calculated across all voxels weighted by WM content

Automated CT-Based Quantification of Microangiopathic Density

Automated CT-based quantification of microangiopathic density in WM was correlated with reference MR-based WML load and Fazekas scores. To obtain CT density exclusive to WM space, we employed a previously introduced algorithm for partial volume tissue segmentation in CT images [12]. In brief, this method is based on probabilistic WM tissue maps in standard space derived from partial tissue segmentations of 600 inconspicuous brain MRIs (3.0 T, T1-3D turbo-field echo) of a population study. The empirical probabilistic WM tissue map was subsequently used for tissue-specific CT segmentation to yield voxel-wise partial WM content. Thus, the algorithm decomposes tissue density (HU) in CT into brain tissue-specific components. The tissue-specific density within WM spaces of the non-ischemic hemisphere was determined by the mean of all voxel densities weighted by WM content (Eq. 1; [12]).

$$\Sigma\,(\mathrm{HU}_{xyz} \times P_{xyz}[\mathrm{WM}]) / \Sigma\,(P_{xyz}[\mathrm{WM}]); \quad (1)$$

HU_{xyz} density of voxel_{xyz}
P_{xyz} partial WM content at voxel_{xyz}

Statistical Analysis

For categorical data, absolute and relative frequencies are given. Univariate distribution of metric variables is described by median and interquartile range.

The following variables were defined:

- VOLWML: MRI-based WML load (in percentage volume of total white matter) as gold standard reference
- Fazekas scores: I = mild, II = moderate, III = severe.
- WMHU: mean CT density (HU) within total white matter (voxel-wise microangiopathic CT density weighted by partial WM content).

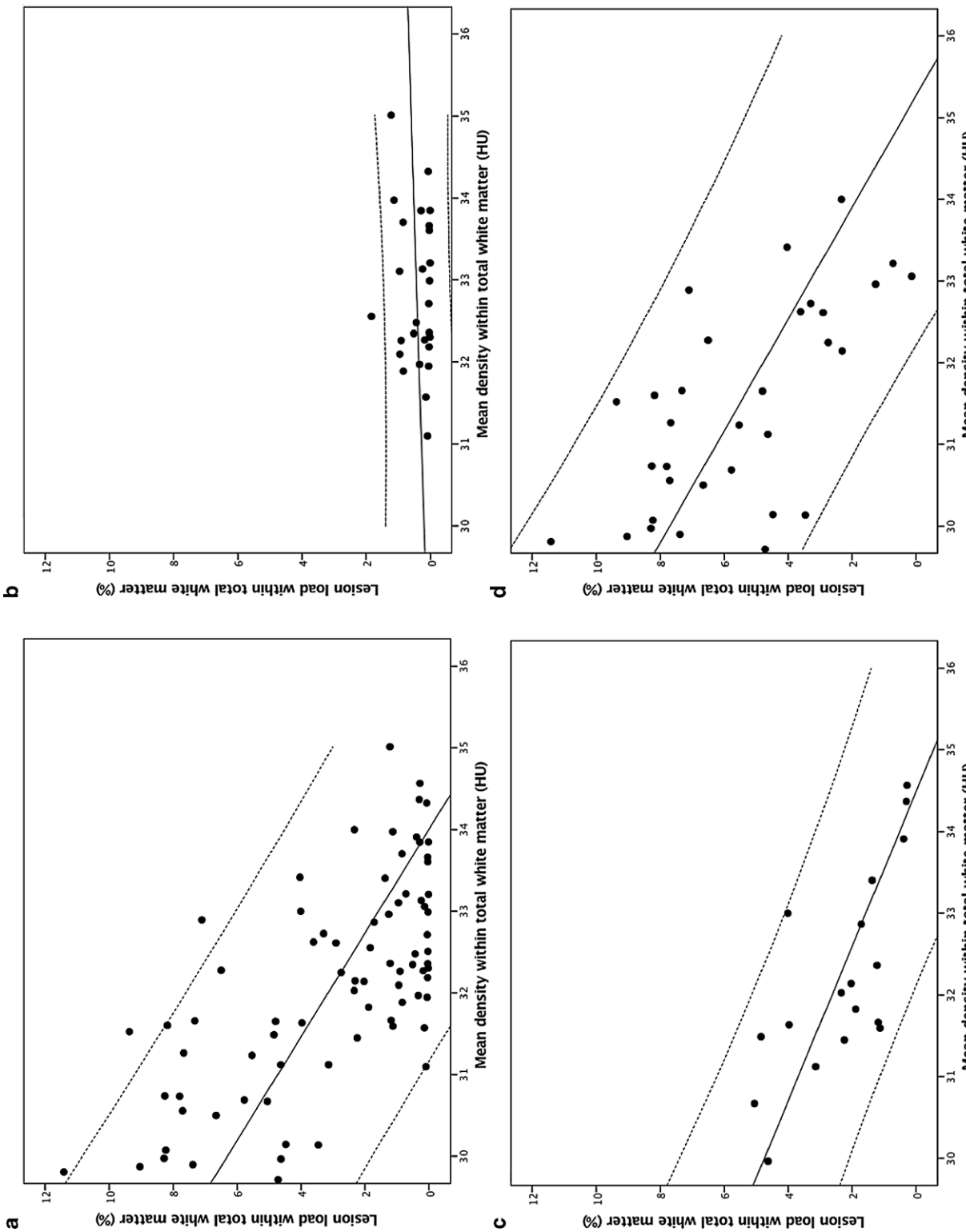

Fig. 2 Mean white matter density (CT) versus WML load (MRI). Correlation between the MR-based WML load within total WM (%) and the mean CT density (HU) within total WM in all patients (r = –0.65) (**a**) and in the different Fazekas score subgroups (Fazekas I, r = –0.002; Fazekas II, r = –0.65; Fazekas III r = –0.52; **b**–**d**, respectively). Linear regression (*solid black line*) and 95% confidence intervals (*dotted lines*) are shown

Table 1 Baseline characteristics of the study population

Characteristic	*n* (%) patients
No. of patients	79
Age, years, median (IQR)	75 (69–82)
Sex, male	50 (63.3%)
Mean CT density within total WM (HU; IQR)	32.2 (31.2–33.0)
WML load within WM (IQR)	1.9% (0.3–4.8%)
Fazekas score	
I	25 (31.6%)
II	23 (29.1%)
III	31 (39.0%)
Time between studies (days, IQR)	1.4 (1.2–2.0)

Given are absolute and relative frequency for categorical variables, median and interquartile range (*IQR*) for metric variables. *NIHSS* National Institutes of Health Stroke scale
MR-based WML load is expressed as percentage within total WM

Spearman correlation was used to quantify association between VOLWML and WMHU in all patients (Fig. 2a) and in the different Fazekas subgroups (Fig. 2b–d).

Two neuroradiologists independently performed Fazekas scoring. For the analyses described, results of the Fazekas score according to the senior neuroradiologist were used. Interrater agreement between both neuroradiologists was measured by Cohen's κ-statistic [15]. Analyses were performed with SPSS version 23 software package (IBM Corporation, Armonk, NY), and are regarded as explorative.

Results

A total of 79 patients with suspected stroke fulfilled the inclusion criteria. The main characteristics of patients are summarized in Table 1. The median MR-based WML load within WM was 1.9% (range 0.3–4.8%) with a minimum lesion load of 0.0% and a maximum of 11.4%. Visual Fazekas scores revealed a varying occurrence of WML among the 79 cases with mild 25 (31.6%), moderate 23 (29.1%) and severe 31 (39.0%) with substantial interrater agreement between the two radiologists (κ = 0.74) (Table 1).

The process of CT-based tissue-specific segmentation was reliable in all 79 cases with a median density within total WM of 32.2 HU (range 31.2–33.0 HU, minimum 29.3 HU, maximum 35.0 HU). Fig. 1b illustrates an example of a tissue-specific decomposition of a CT image in a patient with a high lesion load. The average image processing time of the algorithm was 3:32 min. The CT-based density within WM (expressed in HU) showed a noticeable Spearman correlation (r = –0.65) with VOLWML (expressed as % lesion load of white matter) (Fig. 2a). The Spearman correlation between the WML volume and CT-based density within the Fazekas subgroups revealed a strong diversity (Fazekas I, r = –0.002; Fazekas II, r = –0.65; Fazekas III, r = –0.52) (Fig. 2b–d). After voxel-wise image registration of MRI to CT, we also noticed that pronounced hyperintense WM lesions in MRI are congruent with reduced density in CT, even though there were localized areas of MRI-CT WM lesion mismatch.

In Fazekas subgroup I, the CT-based WMHU does not reliably predict MR-based WML volume with a Spearman correlation coefficient r = –0.002 (Fig. 2b). Consequently, WMHU does not provide additional information in patients with low WML load beyond visual Fazekas scoring. In Fazekas subgroups II and III, however, the CT-based WMHU consistently and reliably predicts MR-based WML volume (Fazekas II, r = –0.65; Fazekas III r = –0.52, Fig. 2c, d); therefore, in patients with moderate or high lesion load according to visual Fazekas score, the CT-based WMHU refines the Fazekas score based prediction of WML load.

Discussion

The presented method [12] allows fully automated observer-independent quantification of voxel-wise WM density in CT with high correlation to the microangiopathic WM disease in gold standard MRI. In patients with moderate or severe WML load according to visual Fazekas score the algorithm provided reliable prediction of MR-based WML load. In the elderly population WML are a common finding and have been strongly associated with increased risk of incident stroke and dementia [16]. They are not only a viable biomarker but also a strong predictor for post-stroke outcomes after thrombectomy and thrombolysis and are related to an increased bleeding risk [4–6, 13]. For that reason, fast and reliable objective assessment of WML load in CT imaging during the acute stroke setting is important and may support decision making in selecting the optimal stroke therapy. The most widely used modality for stroke imaging is CT and there is a need for a fast and objective, rater-independent quantification of WM disease in CT imaging. In contrast to MRI, visual assessment of WM disease in CT imaging is limited in precision and reliability, all the more since HU values do not show a great variance [8, 17]; however, CT offers several advantages over MRI: image acquisition with CT scanners is generally much faster than with MRI and less prone to movement artifacts of agitated stroke patients [18].

The presented fully automated method is based on previously constructed highly refined MR-based tissue probability maps to encode voxel-wise tissue probability in the CT image. The decomposition of Hounsfield units (HU) into tissue-specific components allowed voxel-wise WM specific assessment of CT density. For this reason a quantitative

analysis of segmented tissue can be performed, that is comparable to segmentation of brain MRI [12]. Besides eliminating interrater variability, the presented automated WML segmentation algorithm improved assessment of WML load in CT.

In patients with a visual Fazekas scoring of II (moderate) and III (severe), the CT algorithm enabled a consistent and reliable prediction of WM disease; however, in patients with a Fazekas score of I (mild), WMHU does not provide additional information on MR-based WML volume. Due to the fact that particularly moderate and severe WML loads increase the risk of parenchymal hematoma after thrombectomy in stroke patients [6], a precise prediction of a low lesion load may be less critical; therefore, the quantification of hypodensity within WM space in NCCT is feasible and may be used as a surrogate marker for the severity of WML load as defined by MRI. Pronounced hyperintense WM lesions in MRI were congruent with reduced density in CT on a voxel level, even though there were visible areas of MRI-CT WM lesion mismatch. This finding suggests that the histopathological entity associated with T2 hyperintensity in MRI may be co-localized but not equivalent to the entity associated with density reduction in CT.

Our study has limitations related to its retrospective design with a relatively small cohort size. Stroke patients with an already large hypodense demarcated infarct areal could lead to a falsification of the fully automated calculated WML volume in cerebral CT. Taking the symmetrical distribution of WML into account, in these cases the non-infarcted cerebral hemisphere could be used. The presented results apply to a single center protocol that was tested on one CT scanner only so that further limitations may arise from scanner variability by different vendors and intrinsic detector noise.

The presented method is automated, can be performed on routine CT diagnostic scans, and is therefore suitable for detection and segmentation of WML in large and longitudinal population studies. The robustness of the WMHU parameter with respect to clinical outcome after thrombolysis and/or thrombectomy remains to be confirmed in a non-overlapping prospective cohort of stroke patients.

Conclusion

The presented method allows fully automated observer-independent quantification of microangiopathic WM density in CT with noticeable correlation to volumetric WML load, assessed by the reference standard MRI. This objective surrogate of WML load improves visual WML assessment in CT may support therapeutic decision making during acute stroke triage.

Conflict of interests U. Hanning, P. Sporns, R. Schmidt,T. Niederstadt, J. Minnerup,G. Bier, S. Knecht and A. Kemmling declare that they have no competing interests.

References

1. Basile AM, Pantoni L, Pracucci G, Asplund K, Chabriat H, Erkinjuntti T, Fazekas F, Ferro JM, Hennerici M, O'Brien J, Scheltens P, Visser MC, Wahlund LO, Waldemar G, Wallin A, Inzitari D; LADIS Study Group. Age, hypertension, and lacunar stroke are the major determinants of the severity of age-related white matter changes. The LADIS (Leukoaraiosis and Disability in the Elderly) Study. Cerebrovasc Dis. 2006;21(5–6):315–22.
2. Arsava EM, Rahman R, Rosand J, Lu J, Smith EE, Rost NS, Singhal AB, Lev MH, Furie KL, Koroshetz WJ, Sorensen AG, Ay H. Severity of leukoaraiosis correlates with clinical outcome after ischemic stroke. Neurology. 2009;72(16):1403–10.
3. Ay H, Arsava EM, Rosand J, Furie KL, Singhal AB, Schaefer PW, Wu O, Gonzalez RG, Koroshetz WJ, Sorensen AG. Severity of leukoaraiosis and susceptibility to infarct growth in acute stroke. Stroke. 2008;39(5):1409–13.
4. Curtze S, Melkas S, Sibolt G, Haapaniemi E, Mustanoja S, Putaala J, Sairanen T, Tiainen M, Tatlisumak T, Strbian D. Cerebral computed tomography-graded white matter lesions are associated with worse outcome after thrombolysis in patients with stroke. Stroke. 2015;46(6):1554–60.
5. Curtze S, Haapaniemi E, Melkas S, Mustanoja S, Putaala J, Sairanen T, Sibolt G, Tiainen M, Tatlisumak T, Strbian D. White matter lesions double the risk of post-thrombolytic intracerebral hemorrhage. Stroke. 2015;46(8):2149–55.
6. Shi ZS, Loh Y, Liebeskind DS, Saver JL, Gonzalez NR, Tateshima S, Jahan R, Feng L, Vespa PM, Starkman S, Salamon N, Villablance JP, Ali LK, Ovbiagele B, Kim D, Viñuela F, Duckwiler GR. Leukoaraiosis predicts parenchymal hematoma after mechanical thrombectomy in acute ischemic stroke. Stroke. 2012;43(7):1806–11.
7. Kuller LH, Longstreth WT Jr, Arnold AM, Bernick C, Bryan RN, Beauchamp NJ Jr; Cardiovascular Health Study Collaborative Research Group. White matter hyperintensity on cranial magnetic resonance imaging: a predictor of stroke. Stroke. 2004;35(8):1821–5.
8. Fazekas F, Barkhof F, Wahlund LO, Pantoni L, Erkinjuntti T, Scheltens P, Schmidt R. CT and MRI rating of white matter lesions. Cerebrovasc Dis. 2002;13 Suppl 2:31–6.
9. Maillard P, Delcroix N, Crivello F, Dufouil C, Gicquel S, Joliot M, Tzourio-Mazoyer N, Alpérovitch A, Tzourio C, Mazoyer B. An automated procedure for the assessment of white matter hyperintensities by multispectral (T1, T2, PD) MRI and an evaluation of its between-centre reproducibility based on two large community databases. Neuroradiology. 2008;50(1):31–42.
10. Schmidt P, Gaser C, Arsic M, Buck D, Förschler A, Berthele A, Hoshi M, Ilg R, Schmid VJ, Zimmer C, Hemmer B, Mühlau M. An automated tool for detection of FLAIR-hyperintense white-matter lesions in Multiple Sclerosis. Neuroimage. 2012;59(4):3774–83.
11. Masdeu JC, Irimia P, Asenbaum S, Bogousslavsky J, Brainin M, Chabriat H, Herholz K, Markus HS, Martínez-Vila E, Niederkorn K, Schellinger PD, Seitz RJ; EFNS. EFNS guideline on neuroimaging in acute stroke. Report of an EFNS task force. Eur J Neurol. 2006;13(12):1271–83.
12. Kemmling A, Wersching H, Berger K, Knecht S, Groden C, Nölte I. Decomposing the Hounsfield unit: probabilistic segmentation of brain tissue in computed tomography. Clin Neuroradiol. 2012;22(1):79–91.

13. Zhang J, Puri AS, Khan MA, Goddeau RP Jr, Henninger N. Leukoaraiosis predicts a poor 90-day outcome after Endovascular stroke therapy. AJNR Am J Neuroradiol. 2014;35(11):2070–5.
14. Fazekas F, Chawluk JB, Alavi A, Hurtig HI, Zimmerman RA. MR signal abnormalities at 1.5 T in Alzheimer's dementia and normal aging. AJR Am J Roentgenol. 1987;149(2):351–6.
15. Cohen J. A coefficient of agreement for nominal scales. Educ Psychol Meas. 1960;20(1):37–46.
16. Debette S, Beiser A, DeCarli C, Au R, Himali JJ, Kelly-Hayes M, Romero JR, Kase CS, Wolf PA, Seshadri S. Association of MRI markers of vascular brain injury with incident stroke, mild cognitive impairment, dementia, and mortality: the Framingham Offspring Study. Stroke. 2010;41(4):600–6.
17. Bier G, Bongers MN, Ditt H, Bender B, Ernemann U, Horger M. Enhanced gray-white matter differentiation on non-enhanced CT using a frequency selective non-linear blending. Neuroradiology. 2016;58(7):649–55.
18. Salomon EJ, Barfett J, Willems PW, Geibprasert S, Bacigaluppi S, Krings T. Dynamic CT angiography and CT perfusion employing a 320-detector row CT: protocol and current clinical applications. Klin Neuroradiol. 2009;19(3):187–96.